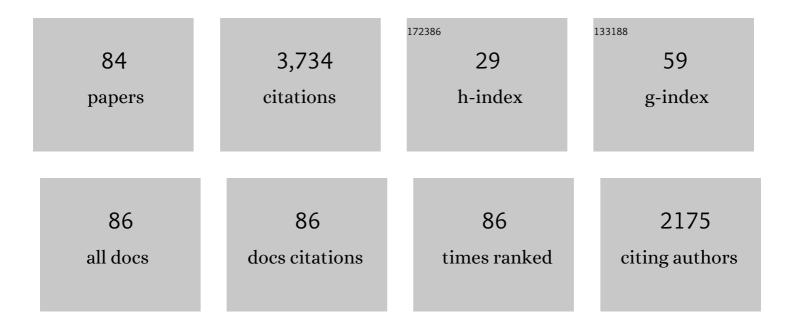
List of Publications by Year in descending order

Source: https://exaly.com/author-pdf/2574456/publications.pdf Version: 2024-02-01



#	Article	IF	CITATIONS
1	Samples returned from the asteroid Ryugu are similar to Ivuna-type carbonaceous meteorites. Science, 2023, 379, .	6.0	97
2	The scientific observation campaign of the Hayabusa-2 capsule re-entry. Publication of the Astronomical Society of Japan, 2022, 74, 50-63.	1.0	6
3	Modeling of 3D trajectory of Hayabusa2 re-entry based on acoustic observations. Publication of the Astronomical Society of Japan, 2022, 74, 308-317.	1.0	5
4	Global Distribution and Geological Context of Coâ€Existing Occurrences of Olivineâ€Rich and Plagioclaseâ€Rich Materials on the Lunar Surface. Journal of Geophysical Research E: Planets, 2022, 127, .	1.5	2
5	Pebbles and sand on asteroid (162173) Ryugu: In situ observation and particles returned to Earth. Science, 2022, 375, 1011-1016.	6.0	78
6	Preliminary analysis of the Hayabusa2 samples returned from C-type asteroid Ryugu. Nature Astronomy, 2022, 6, 214-220.	4.2	136
7	On the origin and evolution of the asteroid Ryugu: A comprehensive geochemical perspective. Proceedings of the Japan Academy Series B: Physical and Biological Sciences, 2022, 98, 227-282.	1.6	77
8	Site selection for the Hayabusa2 artificial cratering and subsurface material sampling on Ryugu. Planetary and Space Science, 2022, 219, 105519.	0.9	4
9	Rotational effect as the possible cause of the east-west asymmetric crater rims on Ryugu observed by LIDAR data. Icarus, 2021, 354, 114073.	1.1	5
10	Thermally altered subsurface material of asteroid (162173) Ryugu. Nature Astronomy, 2021, 5, 246-250.	4.2	47
11	Alignment determination of the Hayabusa2 laser altimeter (LIDAR). Earth, Planets and Space, 2021, 73, .	0.9	3
12	Numerical Simulation of Lunar Seismic Wave Propagation: Investigation of Subsurface Scattering Properties Near Apollo 12 Landing Site. Journal of Geophysical Research E: Planets, 2021, 126, e2020JE006406.	1.5	9
13	Anomalously porous boulders on (162173) Ryugu as primordial materials from its parent body. Nature Astronomy, 2021, 5, 766-774.	4.2	30
14	Light detection and ranging (LIDAR) laser altimeter for the Martian Moons Exploration (MMX) spacecraft. Earth, Planets and Space, 2021, 73, .	0.9	7
15	Improving the geometry of Kaguya extended mission data through refined orbit determination using laser altimetry. Icarus, 2020, 336, 113454.	1.1	8
16	Improving Hayabusa2 trajectory by combining LIDAR data and a shape model. Icarus, 2020, 338, 113574.	1.1	16
17	Hayabusa2 Landing Site Selection: Surface Topography of Ryugu and Touchdown Safety. Space Science Reviews, 2020, 216, 1.	3.7	17
18	Sample collection from asteroid (162173) Ryugu by Hayabusa2: Implications for surface evolution. Science, 2020, 368, 654-659.	6.0	158

#	Article	IF	CITATIONS
19	Highly porous nature of a primitive asteroid revealed by thermal imaging. Nature, 2020, 579, 518-522.	13.7	100
20	Dynamic precise orbit determination of Hayabusa2 using laser altimeter (LIDAR) and image tracking data sets. Earth, Planets and Space, 2020, 72, .	0.9	11
21	Hayabusa2 arrives at the carbonaceous asteroid 162173 Ryugu—A spinning top–shaped rubble pile. Science, 2019, 364, 268-272.	6.0	410
22	The geomorphology, color, and thermal properties of Ryugu: Implications for parent-body processes. Science, 2019, 364, 252.	6.0	313
23	Characteristics of non-tectonic tremors around the Lützow-Holm Bay, East Antarctica, during 2013–2015. Polar Science, 2019, 19, 77-85.	0.5	3
24	Global classification of lunar reflectance spectra obtained by Kaguya (SELENE): Implication for hidden basaltic materials. Icarus, 2019, 321, 407-425.	1.1	8
25	Dust Detection Mode of the Hayabusa2 LIDAR. Space Science Reviews, 2017, 208, 65-79.	3.7	11
26	Albedo Observation by Hayabusa2 LIDAR: Instrument Performance and Error Evaluation. Space Science Reviews, 2017, 208, 49-64.	3.7	13
27	Evidence of impact melt sheet differentiation of the lunar South Poleâ€Aitken basin. Journal of Geophysical Research E: Planets, 2017, 122, 1672-1686.	1.5	22
28	Time–space variations in infrasound sources related to environmental dynamics around Lützow–Holm Bay, east Antarctica. Polar Science, 2017, 14, 39-48.	0.5	8
29	Infrasound Signals and Their Source Location Inferred from Array Deployment in the Lützow-Holm Bay Region, East Antarctica: January-June 2015. International Journal of Geosciences, 2017, 08, 181-188.	0.2	6
30	Seismic Tremors and Their Relation to Cryosphere Dynamics in April 2015 around the Lützow-Holm Bay, East Antarctica. International Journal of Geosciences, 2017, 08, 1025-1047.	0.2	4
31	Development of an application scheme for the SELENE/SP lunar reflectance model for radiometric calibration of hyperspectral and multispectral sensors. Planetary and Space Science, 2016, 124, 76-83.	0.9	33
32	Constraints on timing and magnitude of early global expansion of the Moon from topographic features in linear gravity anomaly areas. Geophysical Research Letters, 2016, 43, 4865-4870.	1.5	6
33	Two-stage development of the lunar farside highlands crustal formation. Planetary and Space Science, 2016, 120, 43-47.	0.9	5
34	Albedo Observation by Hayabusa2 LIDAR: Instrument Performance and Error Evaluation. , 2016, , 49-64.		0
35	Global occurrence trend of high-Ca pyroxene on lunar highlands and its implications. Journal of Geophysical Research E: Planets, 2015, 120, 831-848.	1.5	13
36	Internal structure of the Moon inferred from Apollo seismic data and selenodetic data from GRAIL and LLR. Geophysical Research Letters, 2015, 42, 7351-7358.	1.5	88

#	Article	IF	CITATIONS
37	Featureless spectra on the Moon as evidence of residual lunar primordial crust. Journal of Geophysical Research E: Planets, 2015, 120, 2190-2205.	1.5	13
38	The relative timing of Lunar Magma Ocean solidification and the Late Heavy Bombardment inferred from highly degraded impact basin structures. Icarus, 2015, 250, 492-503.	1.1	30
39	Infrasound array observations in the Lützow-Holm Bay region, East Antarctica. Polar Science, 2015, 9, 35-50.	0.5	13
40	Lunar mare volcanism: lateral heterogeneities in volcanic activity and relationship with crustal structure. Geological Society Special Publication, 2015, 401, 127-138.	0.8	2
41	Infrasound observations at Syowa Station, East Antarctica: Implications for detecting the surface environmental variations in the polar regions. Geoscience Frontiers, 2015, 6, 285-296.	4.3	16
42	Geologic structure generated by largeâ€impact basin formation observed at the South Poleâ€Aitken basin on the Moon. Geophysical Research Letters, 2014, 41, 2738-2745.	1.5	49
43	Quantitative measurement method for impact basin characteristics based on localized spherical harmonics. Icarus, 2014, 228, 315-323.	1.1	2
44	Variation of the lunar highland surface roughness at baseline 0.15–100 km and the relationship to relative age. Geophysical Research Letters, 2014, 41, 1444-1451.	1.5	11
45	Lunar laser topography by LALT on board the KAGUYA lunar explorer – Operational history, new topographic data, peak height analysis of laser echo pulses. Advances in Space Research, 2013, 52, 262-271.	1.2	12
46	Usability of lunar reflectance model based on SELENE/SP for planned HISUI radiometric calibration. , 2013, , .		1
47	Viscoelastic deformation of lunar impact basins: Implications for heterogeneity in the deep crustal paleoâ€thermal state and radioactive element concentration. Journal of Geophysical Research E: Planets, 2013, 118, 398-415.	1.5	22
48	Characteristic atmosphere–ocean–solid earth interactions in the Antarctic coastal and marine environment inferred from seismic and infrasound recording at Syowa Station, East Antarctica. Geological Society Special Publication, 2013, 381, 469-480.	0.8	3
49	A new type of pyroclastic deposit on the Moon containing Feâ€spinel and chromite. Geophysical Research Letters, 2013, 40, 4549-4554.	1.5	38
50	Infrasonic Waves in Antarctica: A New Proxy for Monitoring Polar Environment. International Journal of Geosciences, 2013, 04, 797-802.	0.2	8
51	Infrasound/seismic observation of the Hayabusa reentry: Observations and preliminary results. Earth, Planets and Space, 2012, 64, 655-660.	0.9	16
52	Lunar farside Th distribution measured by Kaguya gamma-ray spectrometer. Earth and Planetary Science Letters, 2012, 337-338, 10-16.	1.8	23
53	Local lunar gravity field analysis over the South Poleâ€Aitken basin from SELENE farside tracking data. Journal of Geophysical Research, 2012, 117, .	3.3	5
54	Compositional evidence for an impact origin of the Moon's Procellarum basin. Nature Geoscience, 2012, 5, 775-778.	5.4	45

#	Article	IF	CITATIONS
55	Olivine-rich exposures in the South Pole-Aitken Basin. Icarus, 2012, 218, 331-344.	1.1	57
56	Massive layer of pure anorthosite on the Moon. Geophysical Research Letters, 2012, 39, .	1.5	102
57	Anomalous Moscoviense basin: Single oblique impact or double impact origin?. Geophysical Research Letters, 2011, 38, n/a-n/a.	1.5	22
58	Timing and characteristics of the latest mare eruption on the Moon. Earth and Planetary Science Letters, 2011, 302, 255-266.	1.8	133
59	Effect of Phase Pattern of Antennas Onboard Flying Spin Satellites on Doppler Measurements. IEEE Transactions on Aerospace and Electronic Systems, 2011, 47, 405-419.	2.6	3
60	Lunar gravity field determination using SELENE same-beam differential VLBI tracking data. Journal of Geodesy, 2011, 85, 205-228.	1.6	63
61	Detection of Acoustic/Infrasonic/Seismic Waves Generated by Hypersonic Re-Entry of the HAYABUSA Capsule and Fragmented Parts of the Spacecraft. Publication of the Astronomical Society of Japan, 2011, 63, 971-978.	1.0	20
62	An Overview of JAXA's Ground-Observation Activities for HAYABUSA Reentry. Publication of the Astronomical Society of Japan, 2011, 63, 961-969.	1.0	21
63	Accuracy assessment of lunar topography models. Earth, Planets and Space, 2011, 63, 15-23.	0.9	9
64	Overview of Differential VLBI Observations of Lunar Orbiters in SELENE (Kaguya) for Precise Orbit Determination and Lunar Gravity Field Study. Space Science Reviews, 2010, 154, 123-144.	3.7	9
65	Illumination conditions of the south pole of the Moon derived using Kaguya topography. Icarus, 2010, 208, 558-564.	1.1	88
66	Possible mantle origin of olivine around lunar impact basins detected by SELENE. Nature Geoscience, 2010, 3, 533-536.	5.4	184
67	An improved lunar gravity field model from SELENE and historical tracking data: Revealing the farside gravity features. Journal of Geophysical Research, 2010, 115, .	3.3	92
68	Same-beam VLBI observations of SELENE for improving lunar gravity field model. Radio Science, 2010, 45, n/a-n/a.	0.8	19
69	Overview of Differential VLBI Observations of Lunar Orbiters in SELENE (Kaguya) for Precise Orbit Determination and Lunar Gravity Field Study. , 2010, , 123-144.		0
70	Lunar Global Shape and Polar Topography Derived from Kaguya-LALT Laser Altimetry. Science, 2009, 323, 897-900.	6.0	263
71	Capability of the penetrator seismometer system for lunar seismic event observation. Planetary and Space Science, 2009, 57, 751-763.	0.9	21
72	Farside Gravity Field of the Moon from Four-Way Doppler Measurements of SELENE (Kaguya). Science, 2009, 323, 900-905.	6.0	169

#	Article	IF	CITATIONS
73	Crustal thickness of the Moon: Implications for farside basin structures. Geophysical Research Letters, 2009, 36, .	1.5	102
74	Mare volcanism in the lunar farside Moscoviense region: Implication for lateral variation in magma production of the Moon. Geophysical Research Letters, 2009, 36, .	1.5	51
75	Same-beam VLBI observation of SELENE. , 2009, , .		1
76	Four-way Doppler tracking for lunar gravity measurements executed by Kaguya and its relay satellite: Okina. , 2009, , .		0
77	Picosecond accuracy VLBI of the two subsatellites of SELENE (KAGUYA) using multifrequency and same beam methods. Radio Science, 2009, 44, .	0.8	38
78	Illumination conditions at the lunar polar regions by KAGUYA(SELENE) laser altimeter. Geophysical Research Letters, 2008, 35, .	1.5	86
79	Analytical and graphical determination of the trajectory of a fireball using seismic data. Planetary and Space Science, 2006, 54, 78-86.	0.9	15
80	The 2003 Kanto large bolide's trajectory determined from shockwaves recorded by a seismic network and images taken by a video camera. Geophysical Research Letters, 2004, 31, .	1.5	26
81	The 1998 Miyako fireball's trajectory determined from shock wave records of a dense seismic array. Earth, Planets and Space, 2003, 55, e9-e12.	0.9	32
82	Azimuthally controlled observation of heavy cosmic-ray primaries by means of the balloon-borne emulsion chamber. Astroparticle Physics, 1997, 6, 155-167.	1.9	21
83	Modeling an international co-operative global complementary production system. Computers and Industrial Engineering, 1994, 27, 205-208.	3.4	2
84	Seismic Wave Interactions Between the Atmosphere - Ocean - Cryosphere System and the Geosphere in Polar Regions. , 0, , .		14